WILEY | Hindawi

Research Article

Magmatic Signature in Submarine Hydrothermal Fluids Vented Offshore Ventotene and Zannone Islands (Pontine Archipelago, Central Italy)

Francesco Italiano,[1] **Davide Romano** ,[1,2] **Cinzia Caruso,**[1] **Manfredi Longo** ,[1] **Andrea Corbo,**[1] **and Gianluca Lazzaro**[1]

[1]*Istituto Nazionale di Geofisica e Vulcanologia, Palermo 90146, Italy*
[2]*Dipartimento di Scienze Matematiche e Informatiche, Scienze Fisiche e Scienze della Terra (MIFT), Università di Messina, Messina 98166, Italy*

Correspondence should be addressed to Davide Romano; dromano@unime.it

Geochemical investigations carried out on submarine hydrothermal fluids vented offshore the Pontine Islands (Tyrrhenian Sea) revealed the existence of gas vents to the W of Zannone Island and SW of Ventotene Island. The geochemical features of the CO_2-rich gas samples show a clear mantle-derived signature with $^3He/^4He$ of 3.72-3.75 Ra and 1.33 Ra at Zannone and Ventotene, respectively. Gas geochemistry denotes how CO_2-rich gases undergo fractionation processes due to CO_2 dissolution to a variable extent favoring enrichment in the less soluble gas species, i.e., CH_4, N_2, and He. The carbon isotope composition of CO_2, expressed as $\delta^{13}C$ vs. V-PDB, ranges from -0.71 and -6.16‰ at Zannone to 1.93‰ at Ventotene. Preliminary geothermometric and geobarometric estimations indicate equilibrium temperatures in the range of 150-200°C at Zannone and >200°C at Ventotene besides H_2O pressures in the range of 5 bar and 20 bar at Zannone and Ventotene, respectively. Although the latest volcanic activity at the Pontine Archipelago is dated Middle Pleistocene, the combination of the new geochemical information along with geothermometric estimations indicates that cooling magmas are likely releasing enough thermal energy to form an efficient hydrothermal system.

1. Introduction

The Central Mediterranean Sea and the Italian Peninsula have been affected by intense Neogene and Quaternary Volcanism. In this sector, the geodynamic processes, framed in the Alpine Orogeny, are expressed by the subduction of the Adriatic microplate under the Eurasian plate and by the opening of the Tyrrhenian back-arc basin [1–4]. These different processes had a prominent role in the genesis, evolution, and migration of partial melts [5–12]. The igneous activity of the Tyrrhenian Sea and its eastern margin triggers the development of several geothermal systems. Hydrothermal fields in the Southern Tyrrhenian Sea are present around seamounts [13–15], in the Aeolian Archipelago [16–19], in front of Capo Vaticano [20, 21], along the coast of Ischia Island

[17], and in the Bay of Naples [22, 23]. All these zones are characterized by CO_2-rich emissions and are commonly associated with the occurrence of magmatic bodies underneath the seafloor. It is accepted that seeping processes are driven by active tectonic lineaments able to control the emission rates and likely responsible for past explosive events [24]. Geochemical features of the thermal fluids provide important information on both the current status of cooling magma batches intruding the upper crust and interaction processes taking place between rising fluids and hosting rocks.

The Pontine Archipelago hosts some examples of submarine geothermal systems connected to a quiescent magmatic activity. The Plio-Pleistocene volcanic rocks from the Pontine Island Volcanoes have a hybrid geochemical
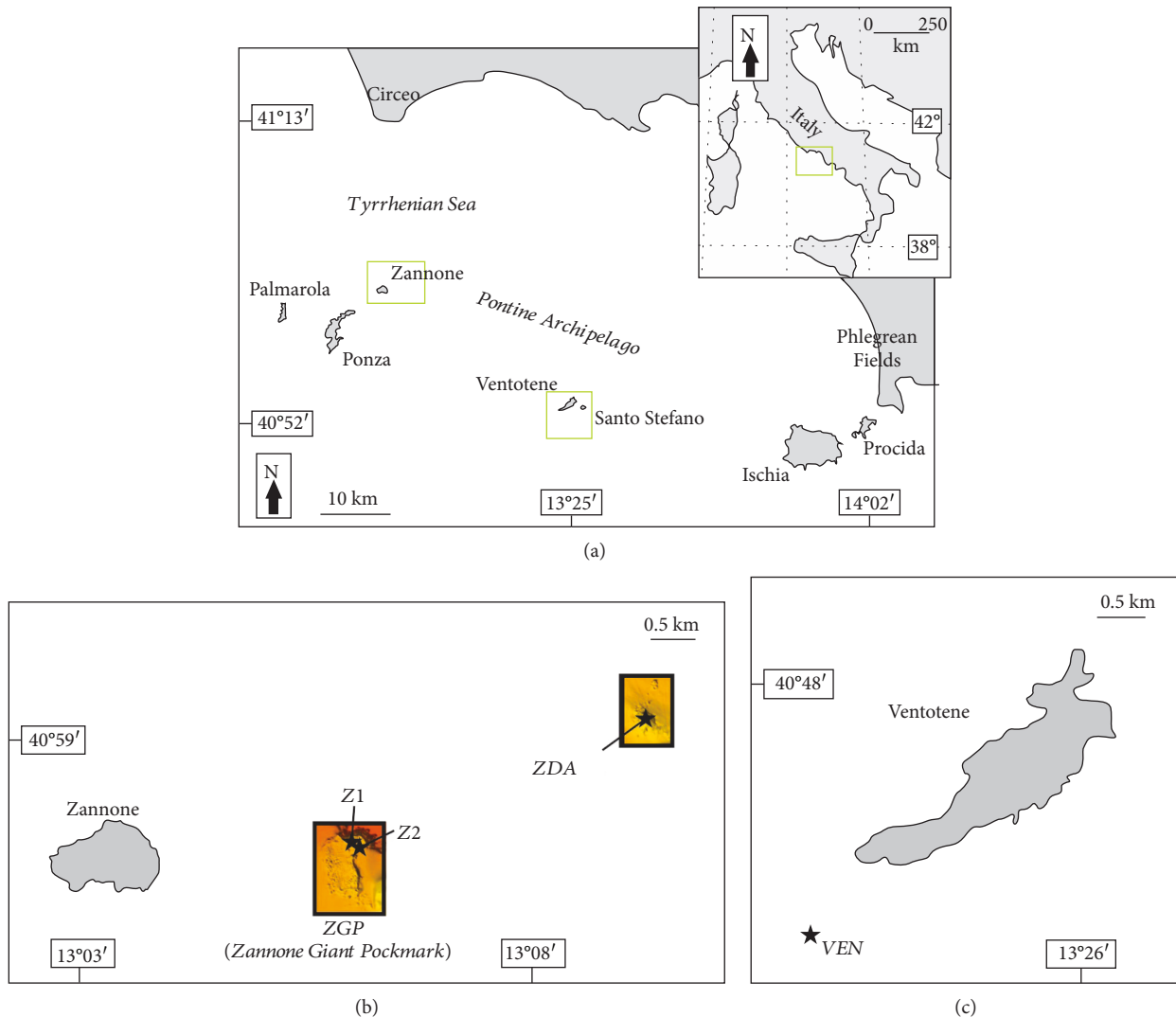
Figure 1: (a) Sketch map of the central Tyrrhenian margin with the location of the areas investigated; (b) location map of the Zannone studied sites (after Martorelli et al. [27]). See Ingrassia et al. [26] and Martorelli et al. [27] for further information; (c) location map of the VEN site lying south to the island of Ventotene.

composition showing island arc and OIB signatures ([9] and references therein). Cadoux et al. [25] pointed out that Pontine Volcanism switched from orogenic magmas emplaced in a syn- to late-collisional context to transitional-type magmas emplaced in a late- to post-collisional stage. The current status of the Pontine Island Volcanism is only expressed by a persistent submarine hydrothermal activity. Several wide and depressed hydrothermal areas have recently been discovered offshore the island of Zannone during morphobathymetric investigations [26, 27] and to the SW of the Ventotene coast during deep diving activity. The hydrothermal activity takes place mainly along NE-SW- and NW-SE-oriented tectonic structures, dissecting the Latium and Campanian continental margins in structural highs (e.g., Ponza-Zannone high) and deep sedimentary basins (e.g., Ventotene and Palmarola basins).

Starting from the first constraints provided by the geochemical features of the hydrothermal fluids collected off-shore the Zannone Island during the "Bolle" cruise in 2014, further investigations were carried out by the oceanographic cruise in 2017 with the aim of obtaining useful insights on the submarine hydrothermal systems of the Pontine Islands.

This paper describes and discusses the geochemical features of the submarine hydrothermal fluids discharged offshore the Zannone and Ventotene islands focusing on the geochemical features of the vented gases. The results show how thermal energy of magmatic origin is still available over the archipelago providing significant perspectives for geothermal energy exploration.

2. Geovolcanological and Hydrothermal Settings

The Pontine Archipelago is located in the Central Tyrrhenian Sea, less than 30 km to the west of the Italian coast, and is composed of five major islands, from NW to SE: Palmarola,

Ponza, Zannone, Ventotene, and Santo Stefano (Figure 1(a)). The volcanic rocks are emplaced over a metamorphic basement overlaid by a Meso-Cenozoic sedimentary succession made up of Late Triassic to Eocene clays, dolostones, limestones, and marls, followed by Miocene flysch deposits [28, 29]. Over the whole archipelago, the prevolcanic substratum only crops out in the northeastern side of Zannone Island [29]. The compressive stress regime has driven the development of a north to northeast verging fold-thrust belt made of a pile of nappes [28]. Starting from the Plio-Pleistocene age, the Alpine belt underwent an extensional deformation [1, 30–32], which has alternatively been interpreted as either a back-arc extension related to an ongoing subduction [33] or as a consequence of a hot asthenosphere flow resulting from the cessation of Adriatic plate subduction [34] or as a divergent plate boundary [35].

The archipelago consists of two different sectors: the northwestern (including Ponza, Palmarola, and Zannone Islands) and the southeastern (including Ventotene and Santo Stefano Islands). The volcanic rocks from the northwestern group display several differences in terms of age and composition in contrast to the rocks forming the southeastern group. Ponza, Palmarola, and Zannone are characterized by the emplacement of calc-alkaline and peralkaline rhyolites showing an age of 4.2 to 1.5 Ma [25]. Only the island of Ponza exhibits a 1.0 Ma old trachytic episode [25, 36–38]. The Pleistocene trachytes are K-alkaline in composition and show a close similarity to the Campanian and Ernici-Roccamonfina products [8, 9, 25, 37]. Paone [39] suggested that calc-alkaline and peralkaline rhyolites were originated from partial melting of a mafic lower crust. On the contrary, Conte et al. [40] indicated that they were derived by fractional crystallization processes of basic orogenic magmas derived from a metasomatised mantle source. The volcanic products include lava flows, domes, and hydromagmatic tuffs.

During the Middle Pleistocene, the volcanic activity shifted eastward to the Ventotene-Santo Stefano area. The development of the two edifices was accompanied by a compositional change. They are indeed mainly represented by basalts and trachybasalts, with minor quantities of shoshonites, latites, and phonolites [9]. They show an age of 0.8-0.13 Ma [41, 42] and are made of lava flows, domes, and pyroclastic materials as fallout, flow, and surge deposits. Pyroclastics are characterized by the presence of sialic, mafic, and ultramafic xenoliths [43].

Submarine hydrothermal systems were recently identified off the islands of Zannone and Ventotene. Off the coast of Zannone, active venting of hydrothermal fluids is located in the northwestern and in the eastern sectors of the insular shelf (Figure 1(b)). Their spatial distribution suggests an active role of the NE-SW-oriented faults affecting the Tyrrhenian offshore of the Latium and Campanian regions. The hydrothermal fields are large depressions up to 10-15 m deep, lying between 110 and 150 m water depth marked by an NNW-SSE elongated shape interpreted as the coalescence of craters connected to explosive events [26]. The depressions developed on sandy wedges considered as low-stand deposits are topped by a thin layer made of mud-sand deposits of the
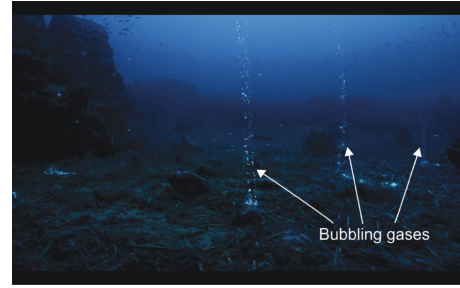

FIGURE 2: Bubbling gases and white patches associated with warm waters vented off Ventotene Island. The hydrothermal fluids occur on a flat area, in water depth varying from 80 to 85 m.

TABLE 1: Location and information of the collected samples. The coordinate reference system is UTM WGS84 zone 33 N.

Site	Locality	Date	Depth (m)	North	East
Z1	Zannone	Feb 2017	134	4537446	340310
Z2	Zannone	Feb 2017	127	4537416	340409
ZDA	Zannone	Feb 2017	147	4539421	345021
VEN	Ventotene	Aug 2018	80	4515668	365025

Holocene age. The hydrothermal fluids are vented all over the depressions and consist of both bubbling gas and thermal water discharges.

An unknown hydrothermal area was discovered off the southwestern coast of Ventotene at a depth of 80 m by diving activity (Figure 1(c)), revealing the presence of bubbling gases. The area was characterized by the presence of warm waters seeping through the seafloor as shown by white patches of bacterial mats made of sulfur precipitates, as well as by several mounds and cones covered by hydrothermal oxides and sulphides (Figure 2). The volcanic rocks outcropping at the seafloor consist of a porphyritic volcanic rock with olivine and pyroxene phenocrysts set in an altered groundmass (Di Bella M., personal communication).

3. Sampling and Analytical Methods

During the 2017 cruise, three vertical casts for water column profiles were carried out using a rosette equipped with a CTD (Conductivity Temperature Depth) and Niskin bottles. Locations and coordinates (UTM-WGS84) of the sites studied are listed in Table 1 and plotted in Figure 1. Fourteen marine water samples were collected from different depths and at the sea bottom (see Tables 1 and 2) for geochemical analyses of the circulating waters and the dissolved gases. Two thermal water samples were collected using a Remote Operated Vehicle (ROV) by a syringe operated by the ROV arm, by inserting a syringe directly into the vent and sucking the water. The temperature at the seafloor was measured using a customized INGV waterproof smart temperature sensor, built to directly operate inside the hydrothermal vents up to a depth of 600 m. The water samples were collected in triplicate and stored as "as is

TABLE 2: Chemical analyses of the water samples. Concentrations in mg/l. Local seawater composition is reported for comparison.

Sample ID	Site	Depth (m)	Type	Sampling method	T (°C)	pH	EC (mS/cm)	Li	Na	K	Mg	Ca	F	Cl	Br	SO_4	HCO_3
2	Z1	50	Water column	Niskin	14.5	8.19	45.95	bdl	12189	453	1439	471	bdl	22036	bdl	3118	171
5	Z1	134	Water column	Niskin	14.4	8.04	45.86	bdl	12488	484	1492	503	bdl	21775	bdl	3032	189
9	Z2	127	Water column	Niskin	14.4	8.19	45.84	bdl	12471	486	1487	489	bdl	21874	bdl	2865	189
13	ZDA	120	Water column	Niskin	14.3	8.22	45.78	bdl	12189	476	1454	482	bdl	21904	bdl	2950	171
14	ZDA	147	Water column	Niskin	14.3	8.19	45.78	bdl	12482	481	1479	492	bdl	21977	bdl	2964	171
15	Z2	124	Thermal waters	ROV	60	n.a.	n.a.	bdl	12234	457	1443	465	bdl	22705	bdl	3165	n.a.
16	ZDA	145	Thermal waters	ROV	56	n.a.	n.a.	bdl	12210	450	1438	476	bdl	22302	bdl	3121	n.a.
	Seawater					8.15		0.17	10468	348	1331	411	1.3	18952	65	2648	135

n.a. = not analyzed. bdl = below detection limits (detection limits for Li = 2.12E-02; F = 4.78E-02; Br = 1.91E-01).

sample" (i.e., not filtered and not acidified), filtered (0.45 μm filter), and "filtered and acidified" (HNO_3 Suprapur-grade acid). The samples for dissolved gas analysis were collected directly from the Niskin bottles and stored in 240 ml glass serum-type bottles sealed in the field by silicon/rubber septa using special pliers. All the samples were collected to avoid even the tiniest bubbles to prevent atmospheric contamination and stored on-board upside-down with the necks immersed in water.

The vented gases were collected by Remote Operated Vehicles (ROV) at Zannone and by diving at Ventotene. The gases offshore Zannone areas were collected in 2014 [27] and in 2017 (this work) using a ROV equipped with a gas sampling system made up of four small funnels connected to 240 ml serum-type bottles. The system was fitted to the front of the ROV with the inverted funnels slipped inside the bottle necks (Figure 3). The ROV pilot placed the system over a gas vent, and the funnel allowed the gas bubbles to be driven into the bottle, where the gas accumulated displacing the seawater out of the bottle. At the end of the dive, when the ROV was back to the surface, an operator sealed the bottles with a gas-tight cap when they were still underwater operating on board of a rubber boat. All the samples collected in the serum-type bottles were stored upside-down with the necks submerged in seawater to minimize gas exchanges with the atmosphere through the cap before undergoing laboratory analysis [44]. A deep-sea dive was carried out in August 2018 off the SW Ventotene coast (Figure 1 and Table 1) to collect the bubbling gases directly from the emission points at the seafloor using an inverted funnel connected to two-way glass bottles. The equipment was filled by marine water to avoid any atmospheric contamination; then, the funnel was placed over the venting gas, and the gas sample was collected by water displacement.

One gas sample from Ventotene and two gas samples from Zannone were analyzed.

FIGURE 3: Sampling system for the bubbling gases off Zannone (depth in the range of 120-150 m bsl). The ROV was equipped with a homemade sampling system composed of four small funnels connected to 240 ml serum-type bottles. The system, fitted to the front of the ROV, allows to collect bubbles by placing the funnel on the venting gases (see text for more information).

The chemical and isotope analysis of dissolved and bubbling gases as well as of the collected waters was carried out at the geochemical laboratories of INGV-Palermo. T°C, pH, and electrical conductivity EC in all the marine water samples were determined by on-board measurements. The pH and EC were measured by electronic instruments calibrated in situ using buffer solutions. In the laboratory, the chemical analysis of the major and minor ions was carried out by ion chromatography (Dionex ICS-1100) on both filtered (0.45 μm), acidified (100 ml HNO_3 Suprapur) water samples (Na, K, Mg, and Ca), as well as on untreated samples (F, Cl, Br, and SO_4). The HCO_3 concentration was determined by standard titration procedures with hydrochloric acid.

The chemical composition of the dissolved and bubbling gases was determined by gas chromatography (GC) using an Agilent equipped with a double TCD-FID detector and argon as carrier gas. Typical analytical uncertainties were within ±5%. The bubbling gas samples had been admitted to the GC by a syringe, while the dissolved gases were extracted from the 240 ml water samples after equilibration at constant temperature with a host gas (high-purity argon) injected into the sample bottle through the rubber septum (for further details see [45, 46]).

The He-isotope ratio in the bubbling gases was analyzed by the injection of the gas to the purification line directly from the sample bottles. The isotope composition of dissolved He was analyzed by headspace equilibration, following the method proposed by Italiano et al. [46]. After purification in the high vacuum, He and Ne were then cryogenically separated and admitted into mass spectrometers. The $^3He/^4He$ ratio was determined by a GVI Helix SFT static vacuum mass spectrometer. The $^4He/^{20}Ne$ ratio was evaluated by peak intensities on the same Helix SFT mass spectrometer. Helium isotope composition is expressed as R/R_a, namely, $^3He/^4He$ of the sample versus the atmospheric $^3He/^4He$ ($R_A = 1.386 \times 10^{-6}$). Some values were corrected for the atmospheric contamination of the sample (R_C/R_A) on the basis of the $^4He/^{20}Ne$ ratio [47]. Typical uncertainties in the range of low ^3He samples are within ±5%.

The carbon isotope composition of CO_2 ($\delta^{13}C$) of the bubbling gases was analyzed by a Delta Plus XP IRMS equipped with a Thermo TRACE GC interfaced with Thermo GC/C III. The Thermo TRACE gas chromatograph was equipped with a Poraplot-Q column (30 m × 0.32 mm i.d.), and the oven was held at a constant temperature of 50°C with the flow rate of carrier gas (He 5.6 grade) kept at a constant flux of 0.8 cc/min.

$\delta^{13}C$ values of the total dissolved carbon ($\delta^{13}C_{TDC}$) were measured on 0.2 ml of water sample introduced in bottles where high-purity helium was injected to remove atmospheric CO_2 (Thermo Scientific GasBench II). The device consists of an autosampler tray kept in a thermostatic rack. 150–200 μl of 100% H_3PO_4 was automatically injected into the vials kept at 70°C for 18 h. Then, the temperature of the thermostatic rack was lowered to 25°C, and the carbon isotope composition of CO_2 produced by acidification was analyzed by a Thermo Scientific Delta V Advantage continuous flow mass spectrometer coupled with Thermo Scientific GasBench II. The results are reported as $\delta^{13}C$‰ vs. V-PDB (Vienna-Pee Dee Belemnite) standard; standard deviation of the $^{13}C/^{12}C$ ratio was ±0.15‰.

4. Results

The analytical results including chemical isotopic ratios of helium, carbon, and $^4He/^{20}Ne$ are listed in Tables 2, 3, and 4. Data for local seawater composition are reported as a reference. The hot waters discharged by hydrothermal vents at Zannone show an outlet temperature up to 60°C. The concentration of the major ions (Na^+, K^+, Mg^{2+}, Ca^{2+}, Cl^-, SO_4^{2-}, and HCO_3^-) is particularly high with respect to those of local seawater (Table 2), and Cl is the dominant anion in all samples, with a concentration approximately higher by 10% than seawater.

The composition of the dissolved gases from offshore Zannone is listed in Table 3 and expressed in ccSTP/L (cm^3 at Standard Temperature and Pressure per liter of seawater). The concentrations of dissolved CO_2, CH_4, and CO are orders of magnitude higher than those in the ASSW (air-saturated seawater).

Bubbling gases from the submarine gas vents of Zannone and Ventotene show a dominance of CO_2 with concentrations above 90% by vol (Table 3). The typical atmospheric species O_2 and N_2 display low values: O_2 in the range of 0.16% vol at both localities, whereas the N_2 content increases from 1.4% at Ventotene to 3.4% at Zannone. The CH_4 concentration is below 1%.

The $^3He/^4He$ isotope ratios in the dissolved gases show values similar to those of atmospheric air ($^3He/^4He = 1.386 \times 10^{-6}$). The $^4He/^{20}Ne$ ratio (Table 4) shows a slight deviation from 0.283 which is assumed to be representative for $^4He/^{20}Ne$ in ASSW [48]. The $^4He/^{20}Ne$ ratio of the bubbling gases is above 25 indicating low atmospheric contamination, whereas the R/Ra ($^3He/^4He$ of the sample versus the atmospheric $^3He/^4He$) ratio increases from 1.33 Ra at Ventotene (sample #19) to 3.72-3.75 Ra at Zannone (samples #17 and 18).

The $\delta^{13}C_{CO2}$ values for the bubbling gases from Zannone are -0.71 and -6.16‰ (samples #17 and 18), while those of $\delta^{13}C_{TDC}$ determined in the dissolved gases ranges between -0.35‰ and -1.51‰ (Table 4). In contrast, the bubbling gases from Ventotene (sample #19) display a positive $\delta^{13}C_{CO2}$ value (1.93‰). In this study, the carbon isotope composition of methane was determined in the bubbling gases from Zannone (samples #17 and 18) only, and the recorded values are -45.5 and -44.2‰ (Table 4).

5. Discussion

5.1. Marine and Thermal Waters. The scenario of the hydrothermal fluids vented at the Pontine Island seafloor is very similar in terms of deposits, gas bubbles, and thermal waters seepage to that of the submarine environment of the Aeolian Islands and other hydrothermal systems of the Mediterranean area. As shown by the analytical results, the geochemical features of the waters and gases collected off Zannone and Ventotene are also very similar to those taken off the Greek Islands (e.g., Milos and Kos [49–51]) and the Aeolian Islands (e.g., Panarea [52]).

As already observed, for the thermal waters vented off Panarea Island [52], the water samples from Zannone are enriched in anions and cations with respect to those of the local seawater (Table 2). The distribution of samples in the Na vs. Cl and Na+K vs. Ca diagrams (Figures 4(a) and 4(b)) suggests the existence of a "concentrated seawater," likely related to boiling of seawater heated by the ascending hot gases. The release of calcium and potassium from host rocks, and the consequent concentration increase of those cations into the thermal waters with respect to the local seawater, can be explained by exchange reactions enhanced by H^+ from the acidic volcanic fluids. As an example, a reaction

TABLE 3: Chemical composition of the dissolved (D) and bubbling gases (B).

Sample ID	Site	Depth (m)	Type	Sampling method	He	H_2	O_2	N_2	CO	CH_4	CO_2
1	Z1	20	D	Niskin	bdl	bdl	3.53	9.24	2.69E-05	3.1E-04	0.46
2	Z1	50	D	Niskin	bdl	bdl	3.36	9.66	2.69E-05	3.8E-04	0.48
3	Z1	80	D	Niskin	bdl	1.53E-04	3.79	9.40	2.15E-05	3.8E-04	0.46
4	Z1	100	D	Niskin	bdl	bdl	3.79	9.82	2.85E-05	4.7E-04	0.64
5	Z1	134	D	Niskin	bdl	1.87E-04	3.56	6.66	2.07E-05	3.7E-04	0.53
6	Z2	50	D	Niskin	bdl	bdl	3.74	9.56	1.71E-05	4.7E-04	0.42
7	Z2	80	D	Niskin	bdl	bdl	3.63	9.37	2.85E-05	4.0E-04	0.45
8	Z2	100	D	Niskin	bdl	bdl	4.38	9.49	bdl	3.0E-04	0.42
9	Z2	127	D	Niskin	bdl	bdl	3.55	9.81	2.69E-05	4.6E-04	0.64
10	ZDA	50	D	Niskin	bdl	1.68E-03	4.16	8.06	bdl	6E-05	0.41
11	ZDA	80	D	Niskin	bdl	6.28E-04	4.43	8.93	bdl	1.22E-04	0.43
12	ZDA	100	D	Niskin	bdl	bdl	2.61	6.50	9.11E-05	2.9E-04	0.41
13	ZDA	120	D	Niskin	bdl	1.73E-04	4.62	9.10	3.98E-05	1.5E-04	0.78
14	ZDA	147	D	Niskin	bdl	bdl	4.83	9.84	2.27E-05	4.9E-04	0.73
	ASSW				*4.80E-05*		*4.80*	*9.60*		*1.0E-6*	*0.24*
17	Z2	127	B	ROV	3.12E-03	1.19E-02	0.016	3.410	3.7E-05	0.985	94.62
17 Rec	Z2	127	B	ROV	3.12E-03	1.19E-02	—	3.353	3.7E-05	0.986	94.68
18	Z2	125	B	ROV	5.63E-02	1E-03	15.26	77.57	2.2E-04	9	0.145
18 Rec	Z2	125	B	ROV	1.85E-01	3.28E-03	—	69.31	7.22E-04	29	0.475
19	VEN	80	B	Two-way glass bottle	4.6E-04	bdl	0.18	1.37	1.82E-04	0.163	98.17
11-BT1*	ZGP	129	B	ROV	7.9E-03	7.0E-04			1.9E-04	2.6E-04	50.94
12-BT1*	ZGP	129	B	ROV	8.2E-03	9.0E-04			1.3E-04	2.6E-04	55.08
13-BT4*	ZGP	127	B	ROV	5.8E-03	bdl			1.9E-04	1.9E-04	54.22

Dissolved gas concentrations are given in ccSTP per liter of seawater. Bubbling gas composition is expressed in vol%. Values for ASSW (air-saturated seawaters) are reported as reference. bdl = below detection limits (detection limits for He, H_2, and CO in the dissolved gases = 5E-06 ccSTP; detection limits for He and H_2 in the bubbling gases = 2E-06). Rec = recalculated concentrations; see text for details. *Reactive gases and labels after Martorelli et al. [27].

TABLE 4: Helium and carbon isotopic composition of the dissolved (D) and bubbling gases (B). The ^{3}He/^{4}He ratios are normalized to the atmospheric helium isotopic composition and expressed as R/Ra where R is the isotopic ratio of the sample and Ra the atmospheric one.

Sample ID	Site	Depth (m)	Type	Sampling method	R/Ra	He/Ne	R/Ra$_c$	Error	$\delta^{13}C_{CO_2}$	$\delta^{13}C_{CH4}$	$\delta^{13}C_{TDIC}$	$CO_2/^3$He
5	Z1	134	D	Niskin	0.91	0.283	—	0.0152	—	n.a.	-0.52	
9	Z2	127	D	Niskin	0.91	0.316	—	0.0143	—	n.a.	-1.51	
13	ZDA	120	D	Niskin	0.80	0.344	—	0.0140	—	n.a.	-0.35	
14	ZDA	147	D	Niskin	0.87	0.511	—	0.0178	—	n.a.	-0.53	
17	Z2	127	B	ROV	3.72	92.19	3.73	0.0325	-0.71	-45.50	—	5.86$E + 09$
18	Z2	125	B	ROV	3.75	51.78	3.76	0.0302	-6.16	-44.28	—	
19	VEN	80	B	Two-way glass bottle	1.33	25.26	1.34	0.0230	1.93	n.a	—	1.14$E + 11$
11-BT1*	ZGP	129	B	ROV	3.49	7.71	3.60	0.02420	n.a.	-43.70	—	
12-BT1*	ZGP	129	B	ROV	3.50	7.11	3.62	0.02434	n.a.	n.a.	—	
13-BT4*	ZGP	127	B	ROV	3.41	5.47	3.56	0.02395	n.a.	n.a.	—	

R/Ra$_c$ is the ^{3}He/^{4}He ratio corrected for the atmospheric contamination (see text for details). n.a. = not analyzed; * Data and labels after Martorelli et al. [27].

like $1.5KAlSi_3O_8 + H^+ = 0.5KAl_3Si_3O_{10}(OH)_2 + K^+ + 3SiO_2$ is a typical hydrothermal alteration moving potassium from K-feldspars to hydrothermal fluids. Similar alteration reactions involving plagioclase and other minerals of the volcanic rocks are responsible for the enrichment in calcium and sodium [52, 53].
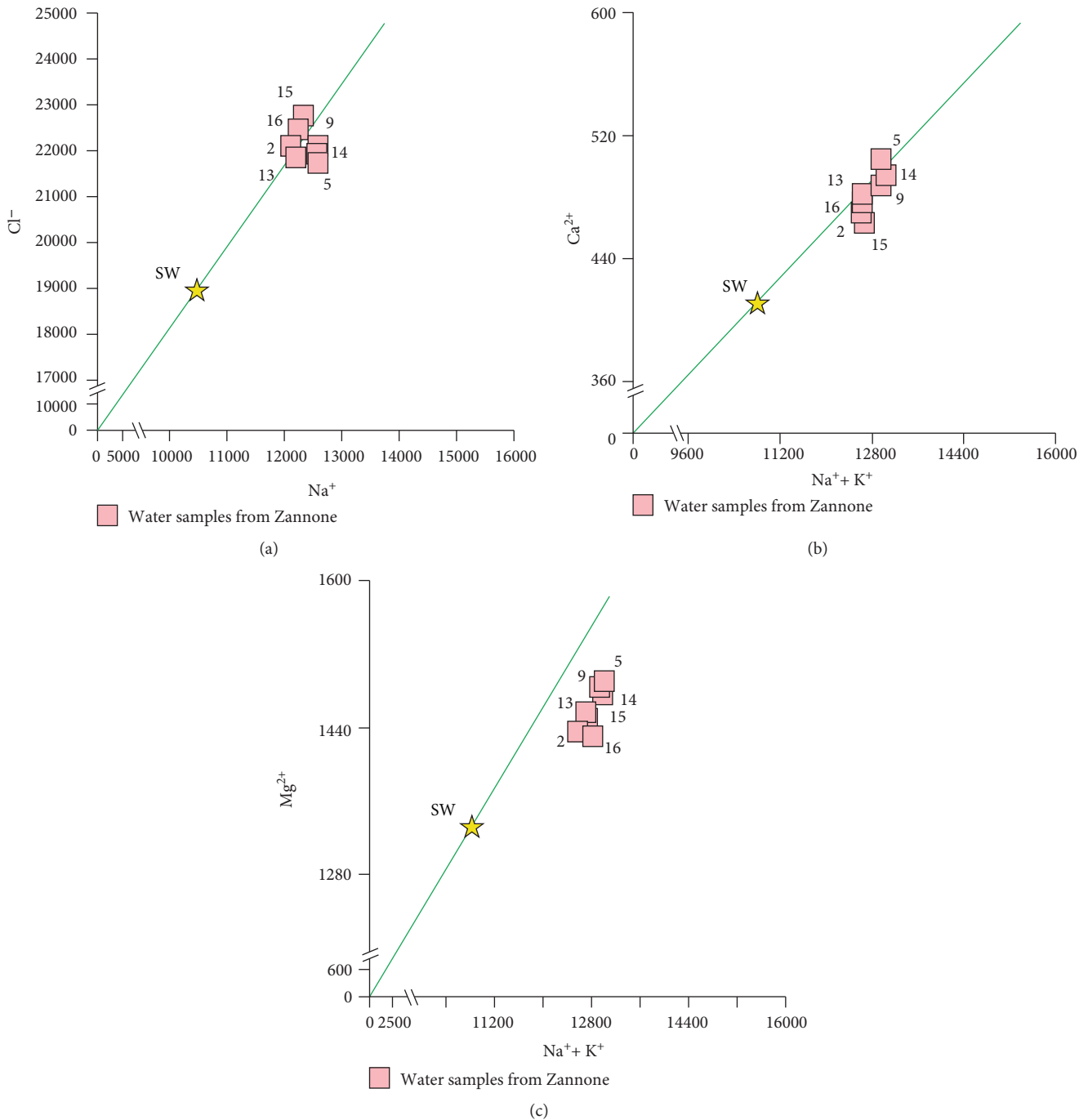
Figure 4: Geochemical features of water samples from Zannone. The star indicates the local seawater. (a) Na vs. Cl (mg/l) binary diagram; (b, c) Ca and Mg vs. Na+K concentrations (mg/l).

The chloride concentration is sometimes higher than that of the local seawater due to phase separation [54] or from the dissolution of magmatic hydrogen chloride [55]. According to the Na+K vs. Mg diagram (Figure 4(c)), the water samples are slightly depleted in magnesium in comparison to a "concentrated seawater" having a Na+K content of around 13000 mg/l. Magnesium is commonly removed from solution when seawater is heated or during high-T reactions with rocks [56, 57]. The general

decrease in magnesium concentration is caused by the formation of Mg-rich secondary minerals during water-rock reactions [58].

Italiano and Nuccio [52] interpreted all the above-mentioned features as a mixing of seawater with thermalized marine waters modified by high-temperature interactions with the hosting rocks and proposed the existence of a deep geothermal system fed by magmatic fluids released by a cooling magma body.
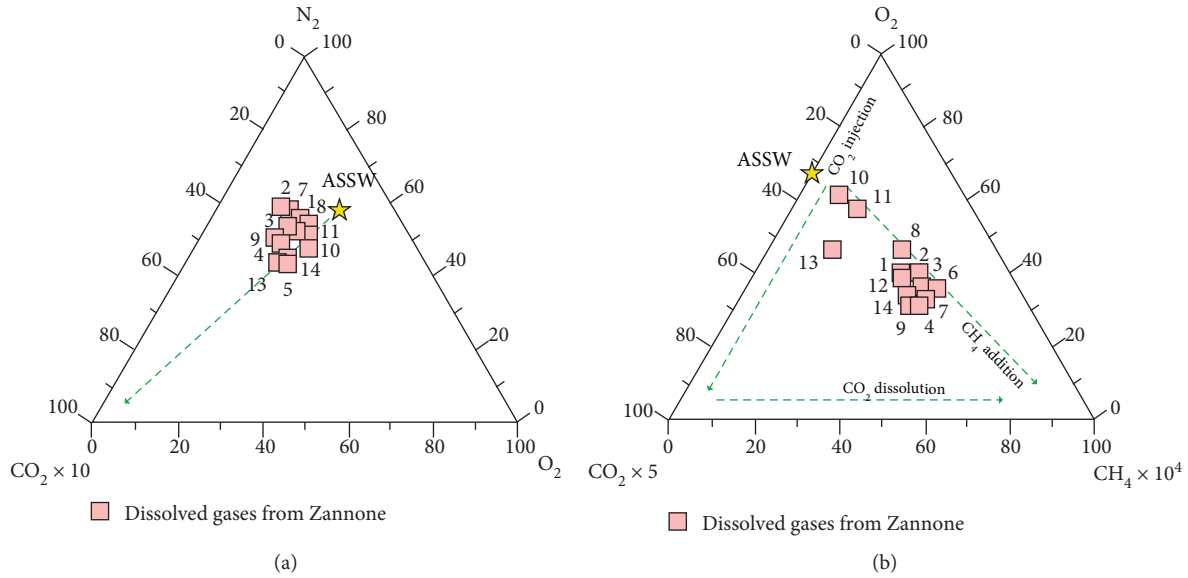
Figure 5: Geochemical relationships for dissolved gases. The star indicates the ASSW (air-saturated seawater). (a) The relative concentrations of CO_2, O_2, and N_2. The dashed line indicates a trend of CO_2 injection in an ASSW; (b) relative concentrations CH_4, O_2, and CO_2. Volcanic/hydrothermal-derived components (CO_2-CH_4) are plotted together with a typical dissolved atmospheric component (O_2). The dashed lines represent trends of CO_2 and CH_4 injection and CO_2 dissolution due to GWI.

5.2. Bubbling and Dissolved Gases. The analytical results for all the dissolved gases from Zannone have been plotted in the CO_2-O_2-N_2 ternary diagram (Figure 5(a)). Samples falling along the ASSW-CO_2 mixing line clearly suggest the presence of a CO_2-rich input. The occurrence of gas-water interaction (GWI) is highlighted in the O_2-CO_2-CH_4 ternary diagram (Figure 5(b)) since samples experienced enrichment in the less soluble species (such as CH_4) along with CO_2 dissolution. Our results for dissolved gases are in agreement with those reported by Martorelli et al. ([27]; see Table 3 and Figure 4).

The bubbling gases were collected by ROV at Zannone (125-127 m depth; Table 3) and by divers at Ventotene (80 m depth). The ROV sampling techniques provided samples with variable atmospheric contamination. Sample #19 taken by divers at Ventotene and one sample (#17) collected by ROV in 2017 at Zannone are CO_2-dominated (94.6-98.1 vol%) and thus denote their magmatic origin as expected. Gas-water interaction (GWI) processes may however affect the final composition of gases collected in the marine environment causing (i) the dissolution of highly soluble species, (ii) CO_2 fractionation, and (iii) enrichment in atmospheric components dissolved in seawater (i.e., N_2 and O_2).

Contrastingly, sample #18 in Table 3 displays high amounts of atmospheric-derived components (O_2 and N_2) associated with a very low CO_2 and high CH_4 and helium contents. Besides the high O_2 and N_2 content, that is related to atmospheric contamination of the sample, the high helium and CH_4 concentrations (564 ppm and 9% by volume, respectively) are worth of notice, as a consequence of a large extent of GWI. Considering that the gases released by hydrothermal systems derive from reducing environments and are thus expected to be O_2 free, we recalculated

their composition subtracting the atmospheric contamination. Assuming that sample #17, after the removal of air contamination, represents the pristine gas concentration, we restored the gas composition considering the concentration ratios of the less soluble gases (He/CH_4, He/N_2). Table 3 displays for gas samples #17 and 18 both the analytical results and the recalculated gas composition (labeled as "Rec").

The isotopic analysis of helium of sample #17 provides a further indication that only the sampling bottle used for the gas-chromatographic analysis suffered an accidental contamination. As shown in Table 4, both samples #17 and 18 display consistent results with high $^4He/^{20}Ne$ ratios denoting negligible air contamination.

5.3. Origin of the Vented Fluids. The helium isotope ratios determined for all the dissolved gases collected within the hydrothermal field off Zannone show atmospheric contamination to variable extents as revealed by the $^4He/^{20}Ne$ ratios close to the atmospheric one (0.283; [48]). On the R/Ra (uncorrected) vs. $^4He/^{20}Ne$ diagram in Figure 6, they cluster very close to the typical ASSW (air-saturated seawater) endmember. On the other hand, the bubbling gases sampled at Ventotene and Zannone suffer a negligible atmospheric contamination as shown by the high $^4He/^{20}Ne$ ratio (>25). The corrected values range from 1.34 at Ventotene (sample #19) to 3.73-3.76 at Zannone (samples #17 and 18), clearly indicating a contribution of mantle-derived He [59]. On the R/Ra (uncorrected) vs. $^4He/^{20}Ne$ diagram (Figure 6), the bubbling gases from Ventotene and Zannone plot in the intermediate zone separating the uncontaminated MORB and the crustal ranges, relatively close to the binary mixing line between an atmospheric and a contaminated mantle source. The $^3He/^4He$ ratio (3.72-3.75 Ra) observed at Zannone (samples #17 and 18) is comparable to those at
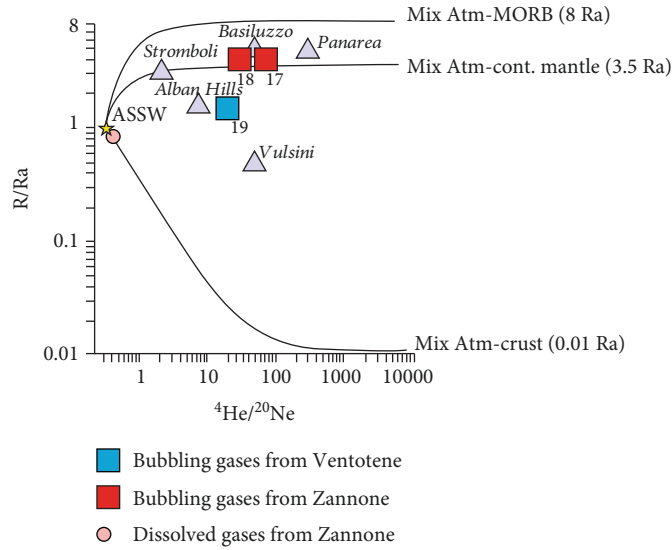
FIGURE 6: Helium isotopic ratios (as R/Ra) and $^4He/^{20}Ne$ relationships. The theoretical black lines represent binary mixing trends for atmospheric helium with helium from crust and mantle sources. The assumed end-members are ASSW (yellow star) with Ra = 1 and He/Ne ratio = 0.267; crust with R/Ra = 0.01 and $^4He/^{20}Ne$ = 5000; MORB-type mantle with R/Ra = 8 and $^4He/^{20}Ne$ = 1000; contaminated mantle by crustal fluids due to subduction of continental crust having Ra = 3.5 and $^4He/^{20}Ne$ = 1000. Data for bubbling gases from Panarea and Basiluzzo [16], Stromboli [60], Vulsini [61], and Alban Hills [62] are plotted for comparison.

Stromboli, Panarea, and Basiluzzo (2.8-4.4 Ra; [16, 60]), while the lower value (1.33 Ra) observed at Ventotene (sample #19) displays a strong affinity with the helium isotope composition of gases from the Roman Comagmatic Province (lower than 2 Ra; [61, 62]). It is worth of notice that the helium isotopic ratios (Table 4) for samples collected off Zannone in 2014 and 2017 provide consistent results with $^3He/^4He$ in the range of 3.56-3.70 Ra that highlight the magmatic contribution to the vented gases. Outcomes from the R/Ra (uncorrected) vs. $^4He/^{20}Ne$ diagram (Figure 6) suggest that the helium isotope composition in the gases from Zannone and Ventotene can be interpreted as a mixture of a mantle and a crustal component or a fractionated He depleted in ^3He because of the long-lasting degassing of the magmatic bodies; however, it denotes the presence of magmatic gases in agreement with the chemical composition.

The carbon isotope composition of methane (in the range from -45.5 to -44.2‰) in the bubbling gases from Zannone (samples #17 and 18) indicates a clear thermogenic derivation ruling out any biogenic contribution. The inorganic origin of the hydrothermal gases is confirmed by the $\delta^{13}C_{CO2}$, being -0.71‰ (sample #17) and -6.16‰ (sample #18) and by the $\delta^{13}C_{TDC}$ of the CO_2 dissolved in the water samples ranging from -1.51‰ to -0.35‰. As CO_2 is a common gas coming from a variety of sources marked by different $\delta^{13}C$ signatures, the typical isotopic signature of the different sources has to be considered. Typical $\delta^{13}C$ values for some of them are organic CO_2 in the range of -24‰ [63], mantle CO_2 $\delta^{13}C$ = -6 ± 2‰ [64], and CO_2 from marine carbonates $\delta^{13}C$ = ~0 ± 2‰ [65]. Moreover, the high reactivity of carbon dioxide and its high solubility in marine waters are responsible fractionation processes able to modify the pristine isotope composition. Therefore, identifying the exact source/sources

involved in the CO_2 production is not always possible using only CO_2 data. According to these limitations, the isotope signature of the CO_2 from Zannone ($\delta^{13}C_{CO2}$ = -0.71 and -6.16‰) could be carefully considered as a mixture of a gaseous contribution derived from a crustal source and a magmatic CO_2 component. The heavier value obtained for the bubbling gases from Ventotene ($\delta^{13}C_{CO2}$ = 1.93‰ ; sample #19) can be interpreted as a stronger contribution of "crustal" CO_2 or, alternatively, it highlights a less GWI during gas uprising. Considering the $CO_2/^3He$ ratios of samples #17 and 19 (Zannone and Ventotene islands; Table 4) besides the $\delta^{13}C_{CO2}$ values, a higher contribution of crustal, probably limestone-type products, can be proposed for gases vented at Ventotene in contrast to a larger contribution of magmatic-type volatiles for Zannone island.

According to Martorelli et al. [27], the mantle component identified in the hydrothermal fluids currently vented offshore Zannon originates in residual magma batches intruded into the crust and never erupted. Direct mantle degassing has been excluded [27] due to permeability limitations induced by the local crustal thickness of about 25 km (see Italiano et al. [66] for further information). Considering that the crustal thickness all along the Tyrrhenian margin of Central Italy is comparable [67], we may also expect that the mantle-derived signature identified at Ventotene is related to the degassing of magma bodies intruded at a relatively shallow crustal level.

With regard to the crustal component, recent studies (i.e., Martelli et al. [68, 69]) pointed out that the Plio-Quaternary volcanic activity from the Roman Comagmatic Province and from the central and eastern sectors of the Aeolian Island reflects an origin in a mantle source contaminated by crustal fluids related to the subduction of the Ionian-Adriatic plate.
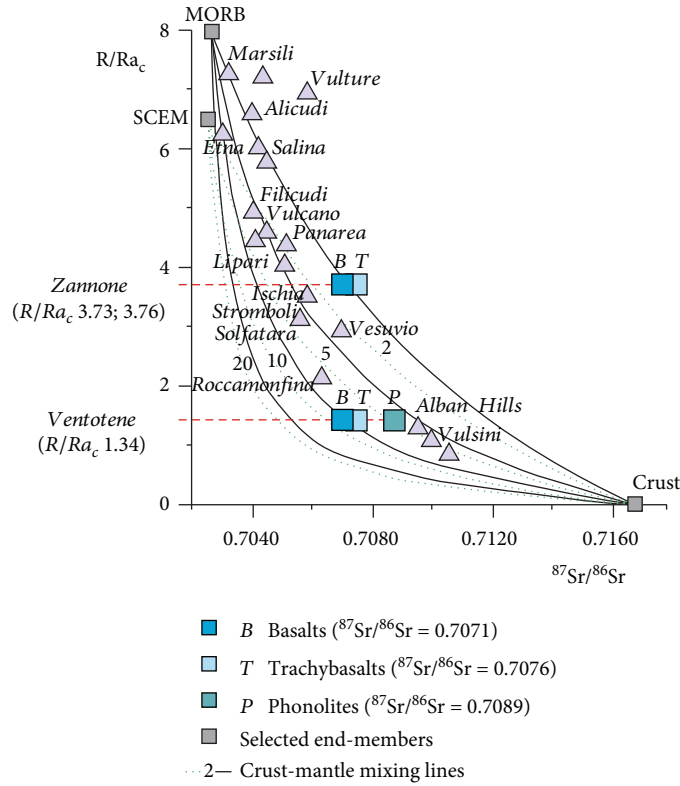
FIGURE 7: $^{87}Sr/^{86}Sr$ versus R/Ra_c for solid and gas samples from the Tyrrhenian area (modified after Martorelli et al. [27]). The lines are binary mixing between MORB-type mantle and SCEM-type mantle (Subcontinental European Mantle; Dunai and Baur [70]) with a crustal end-member. Numbers (2, 5, 10, and 20) indicate the k value ($k = (He/Sr)_{crust}/(He/Sr)_{mantle}$) for each curve. Assumed values for mantle and crust end-members: $^3He/^4He_{radiogenic} = 0.01$ Ra [77]; $^3He/^4He_{MORB} = 8$ Ra [78]; $^3He/^4He_{SCEM} = 6.5$ Ra [70]; $^{87}Sr/^{86}Sr_{radiogenic} = 0.720$ [79]; and $^{87}Sr/^{86}Sr_{asthenosphere} = 0.7030$ [80]. $He_{cont\,crust} = 5 \times 10^{-5}$ cm^3 STP/g [81]; $He_{HIMU} = 5 \times 10^{-7}$ cm^3 STP/g [78]; $Sr_{cont\,crust} = 333$ ppm [82]; and $Sr_{MORB} = 16.4$ ppm [83]. Data after D'Antonio et al. [71], Barberi et al. [72], Martelli et al. [68], and Italiano et al. [15].

Moreover, Conte et al. [40] assumed that the genesis of the Pontine magmas has to be referred to as partial melting processes of a mantle source contaminated by crustal components recycled via subduction. Hence, contamination of the mantle reservoir might be the main factor responsible for the crustal component observed in the hydrothermal fluids.

In order to constrain the magmatic source of the geothermal fluids, the R/Ra_c-$^{87}Sr/^{86}Sr$ diagram (He-Sr relationship) is used (Figure 7). The plot shows binary mixing trends between a crustal end-member and two mantle end-members represented by MORB and SCEM (Subcontinental European Mantle; [70]). He and Sr data from volcanic edifices of the Tyrrhenian area have also been plotted for comparison; most of them refer to values obtained for the same rock sample [15, 68]. The He isotopic ratio observed at Zannone was interpreted [27] as a degassing of cooling mantle-derived magmas having a composition similar to the Pleistocene trachytes (i.e., the Ventotene basalts/trachybasalts). With regard to the hydrothermal fluids emitted SW of Ventotene Island, three different Pleistocene samples belonging to the shoshonitic-type suite outcropping over the island are plotted assuming that those rock types release helium with the same isotopic ratio determined in the bubbling gas ($1.34\,Ra_c$). The Sr isotopic ratios for those rocks are basalts $^{87}Sr/^{86}Sr = 0.70709$ [71], trachybasalts $^{87}Sr/^{86}Sr = 0.70758$ [71], and phonolites $^{87}Sr/^{86}Sr = 0.7089$ [72]. The diagram highlights that the helium isotope ratio of $1.34\,Ra_c$ is consistent with a crust-mantle mixture for all the three Ventotene samples, as they plot within the 5 and 10 binary mixing lines between the values of Roccamonfina and those of the Roman Comagmatic Province (Alban Hills and Vulsini). These results suggest that the Ventotene gases may be deriving from a magmatic source, simply reproducing a crust-mantle mixture. Both basic (basaltic/trachybasaltic) and intermediate magmas (phonolitic) derived from a contaminated mantle source can attain the recorded helium isotopic ratio. Furthermore, they rule out the possibility that the current exhalative activity can be supplied by acidic magmas of anatectic origin.

5.4. Geothermometric and Geobarometric Considerations.

Following the assumption that the submarine hydrothermal fluids vented at Zannone and Ventotene may equilibrate inside a geothermal reservoir at some level beneath the seafloor, we propose the existence of a reservoir kept at boiling conditions by the thermal energy released by cooling magma batches intruded at shallow crustal levels. We constrained the chemical-physical conditions (pressure, temperature,
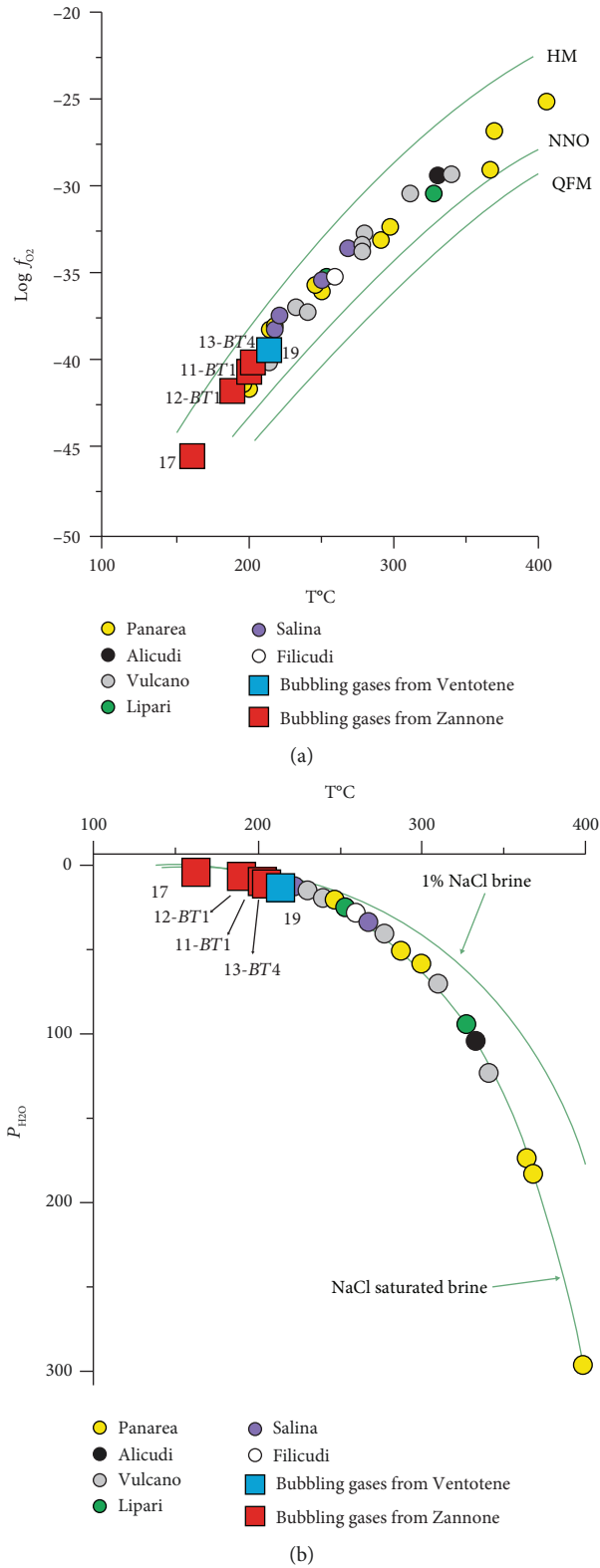
(a)

(b)

FIGURE 8: Geothermometric and geobarometric estimations for the bubbling gases from Zannone and Ventotene (see text and Section 1 of Supplementary Materials for details). B-Z2 and B-VEN were analyzed in this paper; B1, B2, and B3 after Martorelli et al. [27]: (a) temperature vs. oxygen fugacity (expressed as log f_{O_2}) diagram; geothermometric estimations for the submarine hydrothermal systems of the Aeolian Islands are reported for comparison. The solid buffers quartz–fayalite–magnetite (QFM), nickel–nickel oxide (N–NO), and hematite–magnetite (HM) are plotted as reference (after Eugster and Wones [84]). (b) Estimated equilibrium pressure of the hydrothermal reservoirs. The pressure is shown on the vertical axis as P_{H_2O} (bars). The boiling curves for saturated NaCl and 1%NaCl waters (brines) are shown. P_{H_2O} by using the estimated equilibrium temperatures.

and redox) that buffer the chemical composition of the hydrothermal fluids at the reservoir level, using the reactive gases CO, CH_4, and CO_2 as already used for geothermometric and geobarometric estimations in geothermal systems (e.g., Giggenbach [73], Fiebig et al. [74], and references therein) and also for submarine hydrothermal fluids [52]. Among the reactive gases, hydrogen was not considered due to its reactivity that causes unpredictable H_2 losses during fluid upraising.

Giggenbach [75] and Italiano and Nuccio [52] observed how the temperature estimations based on the system H_2O, CO_2, CH_4, and CO assumed to be at boiling conditions are reasonably valid in the range between 100 and 400°C.

In the case of the fluids vented off the Zannone and Ventotene islands, further assumptions and limitations are taken into account as we deal with fluids collected at a depth greater than 120 m bsl. Considering the very high CO_2 solubility in seawater during gas-water interaction (GWI) processes and the observed enrichment of CO and CH_4 (Table 3), we expect that the CO_2/CO and CO_2/CH_4 ratios have been modified during thermal fluid uprise. As observed by Italiano et al. [44], the system adopted is more sensitive to the CO and CH_4 concentrations than that of CO_2, implying that although GWI induces modifications in the chemical composition, the estimated equilibrium temperatures do not change very much even in the case of, even large, CO_2 content changes. The solubility coefficients of CO and CH_4 are similar and about one order of magnitude lower than that of CO_2; thus, they do not alter their abundance ratios (see Section 2 of Supplementary Materials (available here)). Moreover, the slow CO and CH_4 reaction kinetics allows them to keep the deep equilibrium conditions during fluids' upraising. Equations (5) and (6) in Section 1 of Supplementary Materials show how the equilibrium constants are a function of temperature and oxygen fugacity. The water molecule dissociation ($H_2O = H_2 + \frac{1}{2}O_2$) is a function of temperature, and the f_{O2} is buffered by the mineral assemblage (quartz, olivine, hematite, magnetite, and nickel) of the host volcanic rocks.

Only the bubbling gases are considered for the geothermometric estimations, and the results plotted on the already adopted temperature f_{O2} graph (Figure 8(a)) show that even in the case of the Pontine Islands, the samples fall between two theoretical f_{O2} buffers proving that equilibrium is attained at the geothermal system level. The estimations show equilibrium temperatures of 156°C for Zannone (sample #17) and 213°C for Ventotene (sample #19). These results indicate the existence of a geothermal system beneath each of the two islands. The estimated geotemperatures have been used to constrain the depth of the geothermal reservoir, namely, its P_{H2O} according to the T–P_{H2O} relationship for 2 M and NaCl-saturated waters ($\log f_{H2O} = 5.479 - 2047/T$; [76]). P_{H2O} results to be of 5 and 20 bar at Zannone (sample #17) and Ventotene (sample #19), respectively (Figure 8(b)). Moreover, the geothermometric and geobarometric estimations for the bubbling gases collected at Zannone by Martorelli et al. [27] (samples 11-BT1, 12-BT1, and 13-BT4 in Table 3) indicate consistent results

with equilibrium temperatures in the range of 190-200°C and P_{H2O} of 13-18 bars (Figure 8).

6. Concluding Remarks

The Zannone and Ventotene offshore is widely floored by hydrothermal features. Active seeping occurs along regional tectonic lineaments affecting the Central Tyrrhenian continental margin. Faults and fractures create several releasing zones broadly marked by different fluid-escape morphologies such as cones, mounds, and pockmarks. The vented fluids are composed of bubbling gases and hot thermal waters discharged at temperatures up to 60°C. The occurrence of GWI processes, highlighted by the chemical composition of dissolved and bubbling gases, is responsible for the geochemical features of the collected gas phase. Helium and carbon isotope analyses indicate that geothermal fluids are the result of a mixing of mantle and crustal components: the mantle component comes from residual magma batches intruded at shallow crustal depths, whereas the crustal contribution mainly reflects the metasomatism of the upper mantle by crustal fluids recycled via subduction of the Adriatic plate.

Geothermobarometric estimations as well as the chemical composition of fluids collected in the Pontine Archipelago (marine waters, hot thermal waters, and bubbling gases) mark the occurrence of geothermal systems located at various depths beneath the seafloor. The vented thermal waters display the enrichment of major ions in comparison to the local seawater, reflecting mixing of seawater with marine water modified by high-temperature interaction with the hosting rocks. The calculated equilibrium temperatures fall in the range 150-400°C already estimated for the Aeolian Islands (Figure 8). At Zannone and Ventotene, the helium isotopic signature (1.34-3.76 Ra$_c$) clearly indicates a magmatic input probably provided by the same cooling magmatic bodies trapped in the shallow crust that feed the geothermal reservoirs. Our future challenge is to search for brand new hydrothermal features on the seafloor all around the Pontine Islands in order to constrain the total energy budget for the Pontine Archipelago.

Data Availability

The data on gas and water geochemistry used to support the findings of this study are included within the article. In order to strengthen our assumptions, we used some geochemical data from previously reported studies which have been cited.

Conflicts of Interest

The authors declare that there are no conflicts of interest regarding the publication of this paper.

Acknowledgments

Rinaldi for his invaluable discovery and sampling of the gas bubbling of Ventotene.
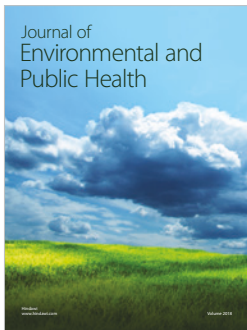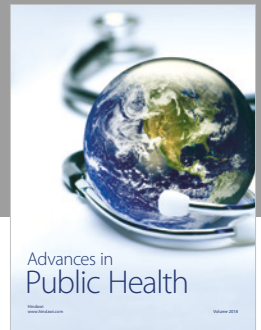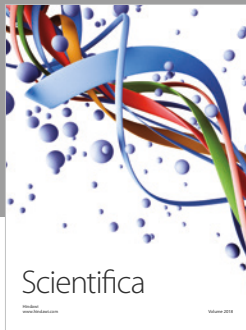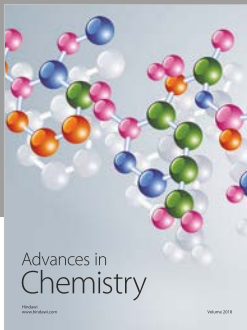
Supplementary Materials

The supplementary materials detail the method applied in this paper to calculate the equilibrium temperatures (Section 1). Moreover, the solubility coefficients of the main species composing the hydrothermal gas emissions are listed in Section 2. *(Supplementary Materials)*

References

[1] A. Malinverno and W. B. F. Ryan, "Extension in the Tyrrhenian Sea and shortening in the Apennines as result of arc migration driven by sinking of the lithosphere," *Tectonics*, vol. 5, no. 2, pp. 227–245, 1986.

[2] L. Jolivet and C. Faccenna, "Mediterranean extension and the Africa-Eurasia collision," *Tectonics*, vol. 19, no. 6, pp. 1095–1106, 2000.

[3] R. Sartori, "The Tyrrhenian backarc basin and subduction of the Ionian lithosphere," *Episodes*, vol. 26, no. 3, pp. 217–221, 2003.

[4] C. Faccenna, C. Piromallo, A. Crespo-Blanc, L. Jolivet, and F. Rossetti, "Lateral slab deformation and the origin of the western Mediterranean arcs," *Tectonics*, vol. 23, no. 1, 2004.

[5] A. Argnani and C. Savelli, "Cenozoic volcanism and tectonics in the southern Tyrrhenian Sea: space-time distribution and geodynamic significance," *Journal of Geodynamics*, vol. 27, no. 4-5, pp. 409–432, 1999.

[6] A. Peccerillo, "Potassic and ultrapotassic magmatism: compositional characteristics, genesis and geologic significance," *Episodes*, vol. 15, no. 4, pp. 243–251, 1992.

[7] A. Peccerillo, "Multiple mantle metasomatism in Central-Southern Italy: geochemical effects, timing and geodynamic implications," *Geology*, vol. 27, no. 4, pp. 315–318, 1999.

[8] A. Peccerillo, Ed., *Plio-Quaternary Volcanism in Italy. Petrology, Geochemistry, Geodynamics*, Springer-Verlag Berlin Heidelberg, 2005.

[9] A. Peccerillo, Ed., *Cenozoic Volcanism in the Tyrrhenian Sea Region*, Springer International Publishing, 2nd edition, 2017.

[10] M. Lustrino, "Phanerozoic geodynamic evolution of the circum-Italian realm," *International Geology Review*, vol. 42, no. 8, pp. 724–757, 2000.

[11] C. Savelli, "Late Oligocene to recent episodes of magmatism in and around the Tyrrhenian Sea: implications for the processes of opening in a young inter-arc basin of intra-orogenic (Mediterranean) type," *Tectonophysics*, vol. 146, no. 1-4, pp. 163–181, 1988.

[12] C. Savelli, "Two-stage progression of volcanism (8–0 Ma) in the Central Mediterranean (southern Italy)," *Journal of Geodynamics*, vol. 31, no. 4, pp. 393–410, 2001.

[13] J. Lupton, C. de Ronde, M. Sprovieri et al., "Active hydrothermal discharge on the submarine Aeolian Arc," *Journal of Geophysical Research*, vol. 116, no. B2, 2011.

[14] S. L. Walker, S. Carey, K. L. Bell et al., *Near-bottom water column anomalies associated with active hydrothermal venting at Aeolian arc volcanoes, Tyrrhenian Sea, Italy*, American Geophysical Union, 2012.

[15] F. Italiano, A. de Santis, P. Favali, M. Rainone, S. Rusi, and P. Signanini, "The Marsili volcanic seamount (southern Tyrrhenian Sea): a potential offshore geothermal resource," *Energies*, vol. 7, no. 7, pp. 4068–4086, 2014.

[16] F. Italiano, "Hydrothermal fluids vented at shallow depths at the Aeolian islands: relationships with volcanic and geothermal systems," *FOG Freiberg Online Geology*, vol. 22, pp. 55–60, 2009.

[17] T. L. Maugeri, G. Bianconi, F. Canganella et al., "Shallow hydrothermal vents in the southern Tyrrhenian Sea," *Chemistry and Ecology*, vol. 26, Supplement 1, pp. 285–298, 2010.

[18] T. Monecke, S. Petersen, M. D. Hannington et al., "Explosion craters associated with shallow submarine gas venting off Panarea island, Italy," *Bulletin of Volcanology*, vol. 74, no. 9, pp. 1937–1944, 2012.

[19] S. Graziani, S. E. Beaubien, S. Bigi, and S. Lombardi, "Spatial and temporal pCO$_2$ marine monitoring near Panarea Island (Italy) using multiple low-cost GasPro sensors," *Environmental Science & Technology*, vol. 48, no. 20, pp. 12126–12133, 2014.

[20] M. Loreto, F. Pepe, R. De Ritis et al., "On the relationships between tectonics and volcanism in the offshore Capo Vaticano, SE Tyrrhenian Sea, during the Plio-Pleistocene," *Rendiconti Online della Società Geologica Italiana*, vol. 31, no. 1, pp. 85–98, 2014.

[21] M. F. Loreto, F. Italiano, D. Deponte, L. Facchin, and F. Zgur, "Mantle degassing on a near shore volcano, SE Tyrrhenian Sea," *Terra Nova*, vol. 27, no. 3, pp. 195–205, 2015.

[22] S. Passaro, S. Genovese, M. Sacchi et al., "First hydroacoustic evidence of marine, active fluid vents in the Naples Bay continental shelf (Southern Italy)," *Journal of Volcanology and Geothermal Research*, vol. 285, pp. 29–35, 2014.

[23] S. Passaro, S. Tamburrino, M. Vallefuoco et al., "Seafloor doming driven by degassing processes unveils sprouting volcanism in coastal areas," *Scientific Reports*, vol. 6, no. 1, article 22448, 2016.

[24] J. Heinicke, F. Italiano, R. Maugeri et al., "Evidence of tectonic control on active arc volcanism: the Panarea-Stromboli tectonic link inferred by submarine hydrothermal vents monitoring (Aeolian arc, Italy)," *Geophysical Research Letters*, vol. 36, no. 4, 2009.

[25] A. Cadoux, D. L. Pinti, C. Aznar, S. Chiesa, and P. Y. Gillot, "New chronological and geochemical constraints on the genesis and geological evolution of Ponza and Palmarola volcanic islands (Tyrrhenian Sea, Italy)," *Lithos*, vol. 81, no. 1-4, pp. 121–151, 2005.

[26] M. Ingrassia, E. Martorelli, A. Bosman, L. Macelloni, A. Sposato, and F. L. Chiocci, "The Zannone Giant Pockmark: first evidence of a giant complex seeping structure in shallow-water, central Mediterranean Sea, Italy," *Marine Geology*, vol. 363, pp. 38–51, 2015.

[27] E. Martorelli, F. Italiano, M. Ingrassia et al., "Evidence of a shallow water submarine hydrothermal field off Zannone Island from morphological and geochemical characterization: implications for Tyrrhenian Sea Quaternary volcanism," *Journal of Geophysical Research: Solid Earth*, vol. 121, no. 12, pp. 8396–8414, 2016.

[28] R. Bartole, D. Savelli, M. Tramontana, and F. C. Wezel, "Structural and sedimentary features in the Tyrrhenian margin off Campania, southern Italy," *Marine Geology*, vol. 55, no. 3-4, pp. 163–180, 1984.

[29] D. De Rita, R. Funiciello, D. Pantosti, F. Salvini, A. Sposato, and M. Velonà, "Geological and structural characteristics of

the Pontine Islands (Italy) and implications with the evolution of the Tyrrhenian margin," *Memorie della Societa Geologica Italiana*, vol. 36, no. 7, pp. 55–65, 1986.

[30] N. Zitellini, M. Marani, and A. Borsetti, "Post-orogenic tectonic evolution of Palmarola and Ventotene basins (Pontine Archipelago)," *Memorie della Societa Geologica Italiana*, vol. 27, pp. 121–131, 1984.

[31] M. I. Marani, M. A. Taviani, F. A. Trincardi, A. Argnani, A. M. Borsetti, and N. Zitellini, "Pleistocene progradation and post-glacial events of the NE Tyrrhenian continental shelf between the Tiber river delta and Capo Circeo," *Memorie della Societa Geologica Italiana*, vol. 36, pp. 67–89, 1986.

[32] M. Marani and N. Zitellini, "Rift structures and wrench tectonics along the continental slope between Civitavecchia and C. Circeo," *Memorie della Societa Geologica Italiana*, vol. 35, no. 2, pp. 453–457, 1986.

[33] A. Frepoli and A. Amato, "Contemporaneous extension and compression in the Northern Apennines from earthquake fault-plane solutions," *Geophysical Journal International*, vol. 129, no. 2, pp. 368–388, 1997.

[34] L. Carmignani and R. Kligfield, "Crustal extension in the northern Apennines: the transition from compression to extension in the Alpi Apuane core complex," *Tectonics*, vol. 9, no. 6, pp. 1275–1303, 1990.

[35] S. Stein and G. F. Sella, "Pleistocene change from convergence to extension in the Apennines as a consequence of Adria microplate motion," in *The Adria Microplate: GPS Geodesy, Tectonics and Hazards*, N. Pinter, G. Gyula, J. Weber, S. Stein, and D. Medak, Eds., vol. 61 of Nato Science Series: IV: Earth and Environmental Sciences, pp. 21–34, Springer, Dordrecht, Netherlands, 2006.

[36] F. Bellucci, M. Grimaldi, L. Lirer, and A. Rapolla, "Structure and geological evolution of the island of Ponza, Italy: inferences from geological and gravimetric data," *Journal of Volcanology and Geothermal Research*, vol. 79, no. 1-2, pp. 87–96, 1997.

[37] A. M. Conte and D. Dolfi, "Petrological and geochemical characteristics of Plio-Pleistocene volcanics from Ponza Island (Tyrrhenian Sea, Italy)," *Mineralogy and Petrology*, vol. 74, no. 1, pp. 75–94, 2002.

[38] E. Martorelli, F. L. Chiocci, A. M. Conte, M. Bellino, and A. Bosman, "Affioramenti vulcanici sottomarini dell'Arcipelago Pontino occidentale: caratteri petrologici e morfoacustici," in *GEOITALIA 2003: 4 Forum Italiano di Scienze Della Terra - Federazione Italiana di Scienze Della Terra*, pp. 16–18, Bellaria, Italia, 2003.

[39] A. Paone, "Petrogenesis of trachyte and rhyolite magmas on Ponza Island (Italy) and its relationship to the Campanian magmatism," *Journal of Volcanology and Geothermal Research*, vol. 267, pp. 15–29, 2013.

[40] A. M. Conte, C. Perinelli, G. Bianchini, C. Natali, E. Martorelli, and F. L. Chiocci, "New insights on the petrology of submarine volcanics from the Western Pontine Archipelago (Tyrrhenian Sea, Italy)," *Journal of Volcanology and Geothermal Research*, vol. 327, pp. 223–239, 2016.

[41] N. Métrich, *Mecanismes d'evolution a l'origine des magmas potassiques d'Italie centrale et meridionale. Exemples du Mt. Somme-Vesuve, des Champs Phlegreens et de l'Ile de Ventotene*, [Ph.D. thesis], University Paris-Sud, Orsay, 1985.

[42] N. Metrich, R. Santacroce, and C. Savelli, "Ventotene, a potassic quaternary volcano in central Tyrrhenian Sea," *Rendiconti della Società Italiana di Mineralogia e Petrologia*, vol. 43, pp. 1195–1213, 1988.

[43] B. De Vivo, K. Torok, R. A. Ayuso, A. Lima, and L. Lirer, "Fluid inclusion evidence for magmatic silicate/saline/CO_2 immiscibility and geochemistry of alkaline xenoliths from Ventotene Island, Italy," *Geochimica et Cosmochimica Acta*, vol. 59, no. 14, pp. 2941–2953, 1995.

[44] F. Italiano, A. Sasmaz, G. Yuce, and O. O. Okan, "Thermal fluids along the East Anatolian Fault Zone (EAFZ): geochemical features and relationships with the tectonic setting," *Chemical Geology*, vol. 339, pp. 103–114, 2013.

[45] F. Italiano, P. Bonfanti, M. Ditta, R. Petrini, and F. Slejko, "Helium and carbon isotopes in the dissolved gases of Friuli region (NE Italy): geochemical evidence of CO_2 production and degassing over a seismically active area," *Chemical Geology*, vol. 266, no. 1-2, pp. 76–85, 2009.

[46] F. Italiano, G. Yuce, I. T. Uysal, M. Gasparon, and G. Morelli, "Insights into mantle-type volatiles contribution from dissolved gases in artesian waters of the Great Artesian Basin, Australia," *Chemical Geology*, vol. 378-379, pp. 75–88, 2014.

[47] Y. Sano and H. Wakita, "Precise measurement of helium isotopes in terrestrial gases," *Bulletin of the Chemical Society of Japan*, vol. 61, no. 4, pp. 1153–1157, 1988.

[48] J. Holocher, F. Peeters, W. Aeschbach-Hertig et al., "Experimental investigations on the formation of excess air in quasi-saturated porous media," *Geochimica et Cosmochimica Acta*, vol. 66, no. 23, pp. 4103–4117, 2002.

[49] P. R. Dando, D. Stüben, and S. P. Varnavas, "Hydrothermalism in the Mediterranean Sea," *Progress in Oceanography*, vol. 44, no. 1-3, pp. 333–367, 1999.

[50] W. D'Alessandro, K. Daskalopoulou, S. Calabrese, M. Longo, K. Kyriakopoulos, and A. L. Gagliano, "Gas geochemistry and preliminary CO_2 output estimation from the island of Kos (Greece)," in , Article ID 17332*EGU General Assembly Conference Abstracts*, vol. 19, Vienna, Austria, 2017.

[51] K. Daskalopoulou, A. L. Gagliano, S. Calabrese et al., "Gas geochemistry and CO_2 output estimation at the island of Milos, Greece," *Journal of Volcanology and Geothermal Research*, vol. 365, pp. 13–22, 2018.

[52] F. Italiano and P. M. Nuccio, "Geochemical investigations of submarine volcanic exhalations to the east of Panarea, Aeolian Islands, Italy," *Journal of Volcanology and Geothermal Research*, vol. 46, no. 1-2, pp. 125–141, 1991.

[53] F. Italiano and C. Caruso, "Detection of fresh and thermal waters over an island with extinct volcanism: the island of Salina (Aeolian arc, Italy)," *Procedia Earth and Planetary Science*, vol. 4, pp. 39–49, 2011.

[54] K. L. Von Damm, L. G. Buttermore, S. E. Oosting et al., "Direct observation of the evolution of a seafloor 'black smoker' from vapor to brine," *Earth and Planetary Science Letters*, vol. 149, no. 1-4, pp. 101–111, 1997.

[55] A. H. Truesdell, J. R. Haizlip, H. Armannsson, and F. D'Amore, "Origin and transport of chloride in superheated geothermal steam," *Geothermics*, vol. 18, no. 1-2, pp. 295–304, 1989.

[56] R. M. Prol-Ledesma, C. Canet, M. A. Torres-Vera, M. J. Forrest, and M. A. Armienta, "Vent fluid chemistry in Bahía Concepción coastal submarine hydrothermal system, Baja California Sur, Mexico," *Journal of Volcanology and Geothermal Research*, vol. 137, no. 4, pp. 311–328, 2004.

[57] E. Valsami-Jones, E. Baltatzis, E. H. Bailey et al., "The geochemistry of fluids from an active shallow submarine hydrothermal system: Milos island, Hellenic volcanic arc," *Journal of Volcanology and Geothermal Research*, vol. 148, no. 1-2, pp. 130–151, 2005.

[58] H. D. Schulz and M. Zabel, Eds., *Marine Geochemistry*, Springer-Verlag Berlin Heidelberg, 2nd edition, 2006.

[59] C. J. Ballentine, R. Burgess, and B. Marty, "Tracing fluid origin, transport and interaction in the crust," *Reviews in Mineralogy and Geochemistry*, vol. 47, no. 1, pp. 539–614, 2002.

[60] S. Inguaggiato and A. Rizzo, "Dissolved helium isotope ratios in ground-waters: a new technique based on gas–water re-equilibration and its application to Stromboli volcanic system," *Applied Geochemistry*, vol. 19, no. 5, pp. 665–673, 2004.

[61] A. Minissale, W. C. Evans, G. Magro, and O. Vaselli, "Multiple source components in gas manifestations from north-central Italy," *Chemical Geology*, vol. 142, no. 3-4, pp. 175–192, 1997.

[62] M. L. Carapezza and L. Tarchini, "Accidental gas emission from shallow pressurized aquifers at Alban Hills volcano (Rome, Italy): geochemical evidence of magmatic degassing?," *Journal of Volcanology and Geothermal Research*, vol. 165, no. 1-2, pp. 5–16, 2007.

[63] P. Deines, D. Langmuir, and R. S. Harmon, "Stable carbon isotope ratios and the existence of a gas phase in the evolution of carbonate ground waters," *Geochimica et Cosmochimica Acta*, vol. 38, no. 7, pp. 1147–1164, 1974.

[64] Y. Sano and B. Marty, "Origin of carbon in fumarolic gas from island arcs," *Chemical Geology*, vol. 119, no. 1-4, pp. 265–274, 1995.

[65] J. Veizer, D. Ala, K. Azmy et al., "$^{87}Sr/^{86}Sr$, $\delta^{13}C$ and $\delta^{18}O$ evolution of Phanerozoic seawater," *Chemical Geology*, vol. 161, no. 1-3, pp. 59–88, 1999.

[66] F. Italiano, M. Martelli, G. Martinelli, and P. M. Nuccio, "Geochemical evidence of melt intrusions along lithospheric faults of the Southern Apennines, Italy: Geodynamic and seismogenic implications," *Journal of Geophysical Research: Solid Earth*, vol. 105, no. B6, pp. 13569–13578, 2000.

[67] A. Minissale, "Origin, transport and discharge of CO_2 in central Italy," *Earth-Science Reviews*, vol. 66, no. 1-2, pp. 89–141, 2004.

[68] M. Martelli, P. M. Nuccio, F. M. Stuart, R. Burgess, R. M. Ellam, and F. Italiano, "Helium–strontium isotope constraints on mantle evolution beneath the Roman Comagmatic Province, Italy," *Earth and Planetary Science Letters*, vol. 224, no. 3-4, pp. 295–308, 2004.

[69] M. Martelli, P. M. Nuccio, F. M. Stuart, V. di Liberto, and R. M. Ellam, "Constraints on mantle source and interactions from He-Sr isotope variation in Italian Plio-Quaternary volcanism," *Geochemistry, Geophysics, Geosystems*, vol. 9, no. 2, 2008.

[70] T. J. Dunai and H. Baur, "Helium, neon, and argon systematics of the European subcontinental mantle: implications for its geochemical evolution," *Geochimica et Cosmochimica Acta*, vol. 59, no. 13, pp. 2767–2783, 1995.

[71] M. D'Antonio, L. Civetta, and P. di Girolamo, "Mantle source heterogeneity in the Campanian region (south Italy) as inferred from geochemical and isotopic features of mafic volcanic rocks with shoshonitic affinity," *Mineralogy and Petrology*, vol. 67, no. 3-4, pp. 163–192, 1999.

[72] F. Barberi, S. Borsi, G. Ferrara, and F. Innocenti, "Contributo alla conoscenza vulcanologica e magmatologica delle Isole dell'Archipelago Pontino," *Memorie della Societa Geologica Italiana*, vol. 6, no. 4, pp. 581–606, 1967.

[73] W. F. Giggenbach, "Geothermal gas equilibria," *Geochimica et Cosmochimica Acta*, vol. 44, no. 12, pp. 2021–2032, 1980.

[74] J. Fiebig, G. Chiodini, S. Caliro, A. Rizzo, J. Spangenberg, and J. C. Hunziker, "Chemical and isotopic equilibrium between CO_2 and CH_4 in fumarolic gas discharges: generation of CH_4 in arc magmatic-hydrothermal systems," *Geochimica et Cosmochimica Acta*, vol. 68, no. 10, pp. 2321–2334, 2004.

[75] W. F. Giggenbach, "Redox processes governing the chemistry of fumarolic gas discharges from White Island, New Zealand," *Applied Geochemistry*, vol. 2, no. 2, pp. 143–161, 1987.

[76] G. Chiodini, L. Marini, and M. Russo, "Geochemical evidence for the existence of high-temperature hydrothermal brines at Vesuvio volcano, Italy," *Geochimica et Cosmochimica Acta*, vol. 65, no. 13, pp. 2129–2147, 2001.

[77] R. K. O'Nions and E. R. Oxburgh, "Helium, volatile fluxes and the development of continental crust," *Earth and Planetary Science Letters*, vol. 90, no. 3, pp. 331–347, 1988.

[78] M. Moreira and M. D. Kurz, "Subducted oceanic lithosphere and the origin of the 'High μ' basalt helium isotopic signature," *Earth and Planetary Science Letters*, vol. 189, no. 1-2, pp. 49–57, 2001.

[79] C. J. Hawkesworth and R. Vollmer, "Crustal contamination versus enriched mantle: $^{143}Nd/^{144}Nd$ and $^{87}Sr/^{86}Sr$ evidence from the Italian volcanics," *Contributions to Mineralogy and Petrology*, vol. 69, no. 2, pp. 151–165, 1979.

[80] B. Marty, T. Trull, P. Lussiez, I. Basile, and J. C. Tanguy, "He, Ar, O, Sr and Nd isotope constraints on the origin and evolution of Mount Etna magmatism," *Earth and Planetary Science Letters*, vol. 126, no. 1-3, pp. 23–39, 1994.

[81] C. J. Allègre, T. Staudacher, and P. Sarda, "Rare gas systematics: formation of the atmosphere, evolution and structure of the Earth's mantle," *Earth and Planetary Science Letters*, vol. 81, no. 2-3, pp. 127–150, 1987.

[82] K. Hans Wedepohl, "The composition of the continental crust," *Geochimica et Cosmochimica Acta*, vol. 59, no. 7, pp. 1217–1232, 1995.

[83] D. R. Hilton, J. A. Hoogewerff, M. J. Van Bergen, and K. Hammerschmidt, "Mapping magma sources in the east Sunda-Banda arcs, Indonesia: constraints from helium isotopes," *Geochimica et Cosmochimica Acta*, vol. 56, no. 2, pp. 851–859, 1992.

[84] H. P. Eugster and D. R. Wones, "Stability relations of the ferruginous biotite, annite," *Journal of Petrology*, vol. 3, no. 1, pp. 82–125, 1962.